

Pentacene Thin Film Transistors Fabricated by High-aspect Ratio Metal Shadow Mask

Sung Hun Jin, Keum Dong Jung, Hyung Chul Shin, Byung-Gook Park, and Jong Duk Lee
Inter-University Semiconductor Research Center (ISRC) and School of Electrical Engineering,

Sang Min Yi and Chong Nam Chu

School of Mechanical and Aerospace Engineering,
Seoul National University, San 56-1, Shinlim-dong, Kwanak-gu, Seoul 151-742, Korea

Tel:02-880-7282, Fax:02-880-7268, e-mail:harin74@dreamwiz.com

Abstract

The robust and large-area applicable metal shadow masks with a high aspect ratio more than 20 are fabricated by a combination of micro-electro-discharge machining (μ -EDM) and electro chemical etching (ECE). After defining S/D contacts using a 100 μ m thick stainless steel shadow mask, the top-contact pentacene TFTs with channel length of 5 μ m showed routinely the results of mobility of 0.498 ± 0.05 cm^2/Vsec , current on/off ratio of 1.6×10^5 , and threshold voltage of 0 V. The straightly defined atomic force microscopy (AFM) images of channel area demonstrated that shadow effects caused by the S/D electrode deposition were negligible. The fabricated pentacene TFTs have an average channel length of 5 ± 0.25 μ m.

1. Introduction

Among various organic semiconductors, pentacene continues to be an attractive material choice because of its high mobility on the order of 1 cm^2/Vsec for a variety of electronic applications, including information display [1-3], electronic paper [4], and radio frequency identification (RFID) [5].

Even though pentacene thin film transistors (TFTs) can be implemented in one of two configurations, i.e., top contact and bottom contact [6], the best performances of pentacene TFTs in the literature [7,8] have been always demonstrated in the top contact configuration due to the inherently favorable conditions of pentacene growth compared with bottom contact mode [6]. However, the top contact mode is incompatible with the conventional photolithography for the definition of source and drain (S/D) electrodes on organic semiconductor due to their intolerance to the exposure of solven-

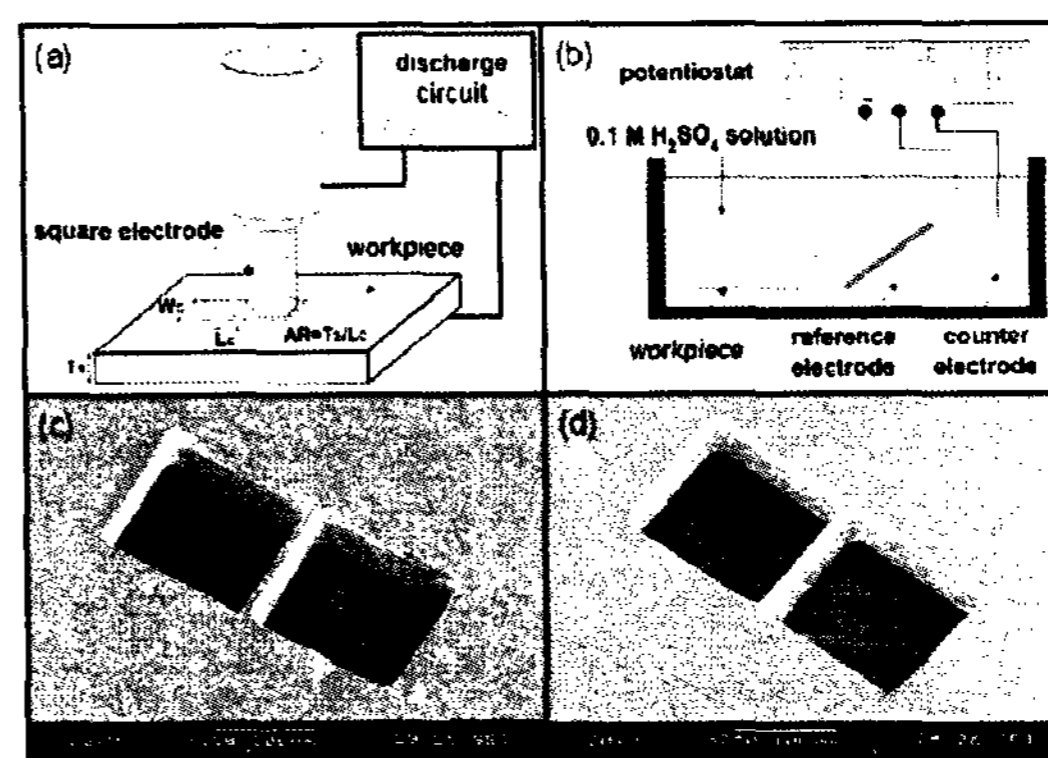


FIG 1. Schematic configurations for (a) micro-electro-discharge machining (μ -EDM) and (b) electro-chemical etching (ECE). The aspect ratio (AR) of an HR shadow mask denotes the ratio of the thickness of workpiece (T_s) to the length of a bridge (L_c). After μ -EDM processing up to the channel length of 10 μ m, the work piece consecutively was electro chemically etched with an etch rate of 4.4 $\text{\AA}/\text{sec}$ in 0.1 mole H_2SO_4 solution (c) A SEM image for a stainless steel shadow mask right after μ -EDM process. After μ -EDM process, L_c is 10 μ m with an aspect ratio of 10 (d) A SEM image for a metal shadow mask right after μ -EDM and ECE process. L_c is 3.6 μ m with an aspect ratio of 28. The width of bridge (W_c) is 150 μ m.

ts and other liquids [9].

Therefore metal shadow masks are generally used to define the top S/D contacts on organic materials because they can guarantee simple S/D definition process without damage of organic materials. But the S/D patterning process by the conventional metal shadow masks ($L_c \approx 20 \sim 70$ μ m) [6], [9] has two major obstacles, which are high resolution patterning

[10] and mass manufacturability. While commercial products like OLED eliminate gradually the pessimistic prospect for the applications of a metal shadow mask to mass production [11], the high resolution patterning using shadow masks can be a remaining barrier on highly integrated top-contact OTFTs [8]. To achieve top-contact OTFTs with a high areal density, several approaches including cold welding [12], high resolution rubber stamping [13] and special Si membrane masks [14] have been reported in the literature, whereas each method has fundamental drawbacks of too much complicated implementation [12], low-level manufacturability for large area applications [13], and easy brittleness [14].

In this work, we proposed and implemented metal shadow masks with a high aspect ratio ($AR > 20$) based on a combination of anisotropic micro-electro-discharge machining (μ -EDM) [15] and isotropic electro chemical etching (ECE) for the application of OTFTs scaled down less than $5 \mu\text{m}$. The high-aspect ratio (HR) metal shadow masks have inherent merits of structural robustness, simple S/D patterning process, and re-usage. In addition, a batch mode μ -EDM technique can be fundamentally applicable to metal shadow masks of a high throughput and good uniformity for a large area application [17].

2. Experiments and Results

Figure 1 presents a schematic illustration of (a) μ -EDM [15] and (b) ECE [16], which were used to fabricate metal shadow masks with high AR larger than 20. As shown in Fig. 1(a), an AR for a metal shadow mask is defined as the thickness of a shadow mask (T_s) to the length of a bridge (L_c). In this experiment, μ -EDM system used the applied voltage of 100 V, a single RC pulse timing circuits with 500 pF and 1 K Ω , and a square copper electrode with one side length of $130 \mu\text{m}$ and structural height of $1500 \mu\text{m}$ fabricated by wire electrode discharge gliding (WEDG)[18]. The work pieces for shadow masks are $100 \pm 5 \mu\text{m}$ thick stainless steel (304 SS) with the size of $1.5 \text{ cm} \times 1.5 \text{ cm}$. After serially machining $150 \mu\text{m}$ square contact holes using μ -EDM, the combinational process of

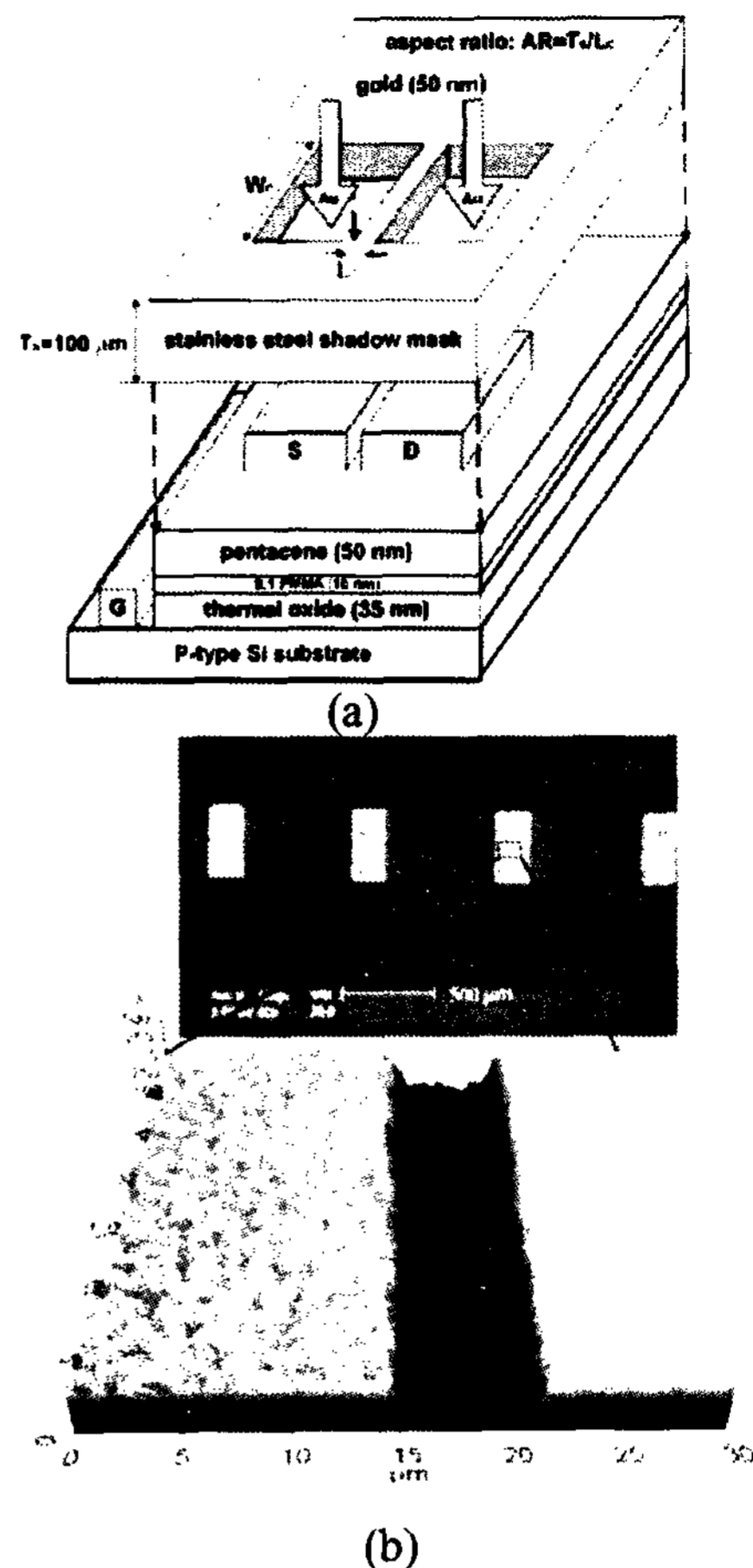


FIG. 2. (a) Schematic illustration of process steps for pentacene TFTs fabricated using an HR metal shadow mask. The width of the wall (L_c) for metal shadow masks ranges from $20 \mu\text{m}$ to $5 \mu\text{m}$ with a fixed channel width of $150 \mu\text{m}$. (b) SEM image of pentacene TFTs with a channel length of $5 \mu\text{m}$ after measurement of electrical characteristics and AFM image of the channel area of a pentacene TFT.

ECE improves the AR of a metal shadow mask noticeably because the μ -EDM has a fundamental limit of the routinely machinable feature size ($L_c \approx 10 \mu\text{m}$) as shown in Fig. 1(c). Figure 1(b) shows that process conditions of ECE system are the applied voltage of 1.2 V and the 0.1 mole H_2SO_4 solution as electrolyte. Figure 1 (c) and (d) showed SEM images for a metal shadow mask after μ -EDM and ECE steps, respectively. To date, the length (L_c) and width (W_c) of the bridge can be routinely obtained as

small as $5 \pm 0.25 \mu\text{m}$ and $70 \pm 1 \mu\text{m}$, respectively.

Figure 2(a) shows a schematic for the fabrication steps of pentacene TFTs. For a gate insulator, 35 nm thick thermal oxide was grown on a p-type wafer with the resistivity of $15 \Omega\text{cm}$. The thermal oxide was patterned by photolithography, and then etched by dilute HF solution for a gate electrode deposition. After cutting the patterned Si wafer to the size of $2 \text{ cm} \times 2 \text{ cm}$, each sample was spin-coated with a dilute PMMA solution to improve the ordering of pentacene due to the hydrophobic ending group methyl radical ($-\text{CH}_3$) [19]. The coated PMMA thickness was 10 nm as measured by ellipsometry. A 50 nm thick pentacene was thermally evaporated on the PMMA treated gate oxide at a rate of about $0.3 \text{ \AA}/\text{sec}$. During the deposition, the substrate temperature maintained at the temperature of $90 \text{ }^\circ\text{C}$ in the pressure of 8×10^{-8} torr. Pentacene was purchased from Aldrich Company, and its purity was about 98 % based on a CHN (carbon, hydrogen, and nitrogen) elemental test. The pentacene source in this experiment was used without purification. Finally 50 nm of gold was e-beam evaporated on pentacene active layer through a $100 \mu\text{m}$ thick HR shadow mask to define S/D contacts as well as the gate contacts. The dimension of source and drain contacts have the channel length ranging from $20 \mu\text{m}$ to $5 \mu\text{m}$ at a fixed channel width of $150 \mu\text{m}$. Figure 2 (b) shows the AFM and SEM image of channel area for an OTFT with $W_c=150 \mu\text{m}$ and $L_c=5 \mu\text{m}$. As shown in Fig. 2 (b), the defined source and drain contacts have a good straight channel.

Figure 3 shows that electrical transfer and output characteristics of pentacene TFTs fabricated by an HR shadow mask with the L_c of $5 \mu\text{m}$ and W_c of $150 \mu\text{m}$. From the transfer characteristics as shown in Fig. 3(a), a saturation mobility of $0.498 \pm 0.05 \text{ cm}^2/\text{Vsec}$, a current on/off ratio of 1.6×10^5 , a subthreshold swing (SS) of $2.5\text{V}/\text{dec}$, and a threshold voltage of 0 V are extracted. The comparatively low level of current on/off ratio and SS are attributed to the periphery areas of pentacene layer, whereas the electrical performances can be improved by removing periphery areas of pentacene [20]. As

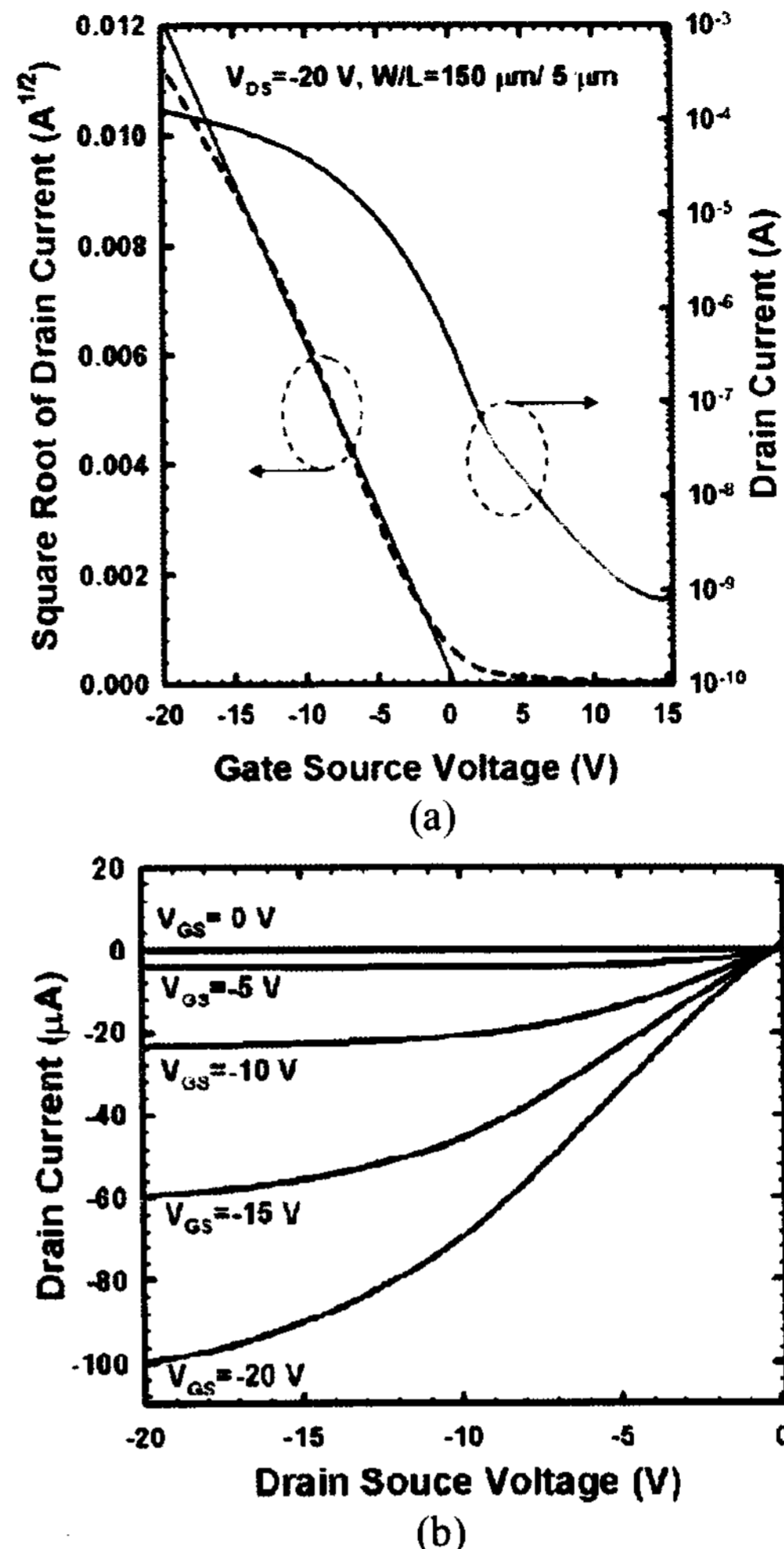


Fig 3. (a) Transfer and (b) output characteristics of a pentacene TFT with the ratio of $W/L=150 \mu\text{m}/5 \mu\text{m}$

shown in Fig. 3(b), a pentacene TFT has the nice saturation characteristics and the saturation current of $100 \mu\text{A}$ at the voltage of $V_{DS} = V_{GS} = -20\text{V}$.

3. Conclusion

We have proposed metal shadow masks with a high aspect ratio ($AR > 20$) using μ -EDM and ECE for high definition of S/D contacts ($L \leq 5 \mu\text{m}$ and $W \leq 150 \mu\text{m}$) on organic semiconductors. The fabricated pentacene TFTs with the channel length of about $5 \mu\text{m}$ showed routinely mobility of $0.498 \pm 0.05 \text{ cm}^2/\text{Vsec}$ and current on/off ratio of 1.6×10^5 . The HR metal shadow masks with high aspect ratio more than

20 can be used repeatedly for S/D electrodes deposition due to the structural robustness. The pentacene TFTs by HR shadow masks can meet the required OELD pixel resolution ($\leq 100 \times 100 \mu\text{m}^2$) as well as high current drivability through the scaling-down of the width of OTFTs [11]. In addition, a batch mode μ -EDM can potentially solve a throughput and yield problem of HR metal shadow mask generation.

4. Acknowledgements

This work was supported by the contract of ISRC(Inter-University Semiconductor Research-Center) 2002-X-5505 to ETRI(Electronics and Telecommunications Research Institute) and MIC (Ministry of Information and Communication) to carry out the Advanced Technology Project.

5. References

- [1] P. Mach, S. J. Rodriguez, R. Nortrup, P. Wiltzius, and J. A. Rogers, *Appl. Phys. Lett.* **78**, 3592 (2001).
- [2] C. D. Sheraw, L. Zhou, J. R. Huang, D. J. Gundlach, T. N. Jackson, M. G. Kane, I. G. Hill, M. S. Hammond, J. Campi, B. K. Greening, J. Francl, and J. West, *Appl. Phys. Lett.* **80**, 1088 (2002).
- [3] H. E. A. Huiteman, G. H. Gelinck, J. B. P. H. van der Putten, K. E. Kuijk, K. M. Hart, E. Cantatore, and D. M. de Leeuw, *Adv. Mater. (Weinheim, Ger.)* **14**, 1201(2002).
- [4] Gerwin H. Gelinck, H. Edzer A, Huitema, Erik Van Veenendaal, Eugenio Cantatore, Laurens Schrijnemakers, Jan B. P. H. Van der Putten, Tom C. T. Geuns, Monique Beenhakkers, Jacobus B. Giesbers, Bart-Hendrik Huisman, Eduard J. Meijer, Estrella Mena Benito, Fred J. Touwslager, Albert W. Marsman, Bas J. E. Van Rens, and Dago M. De Leeuw, *Nature Mat.* **3**, 106 (2004).
- [5] P. F. Baude, D. A. Ender, M. A. Haase, T. W. Kelley, D. V. Muyres, S. D. Theiss, *Appl. Phys. Lett.* **82**, 3964 (2003).
- [6] Ioannis Kymissis, C. D. Dimitrakopoulos, and Sampath Purushothaman, *IEEE Trans. Electron Devices* **48**, 1060 (2001).
- [7] Hagen Klauk, Marcus Halik, Ute Zschieschang, Günter Schmid, and Wolfgang Radlik, *J. Appl. Phys.* **9**, 5259 (2002).
- [8] Paul F. Baude, David A. Ender, Tommie W. Kelley, Michael A. Haase, Dawn V. Muyres, and Steven D. Theiss, 2003 Int. Electr. Dev. Meet. Techn. Dig., 8. 1. 1 (2003).
- [9] D. J. Gundlach and T. N. Jackson, "Solvent-induced phase transition in thermally evaporated pentacene films", *Appl. Phys. Lett.* **74**, 3302 (1999).
- [10] G. J. Burger, E. J. T. Smulders, J. W. Berenschot, T. S. J. Lammerink, *Sensors and Actuators A* **54**, 669 (1996).
- [11] E. Becker, T. Riedl, T. Dobbertin, D. Schneider, D. Heithecker, D. Metzdorf, H. H. Johannes, and W. Kowalsky, *Appl. Phys. Lett.* **82**, 2712 (2003).
- [12] Changsoon Kim, Max Shtein, and Stephen R. Forrest, *Appl. Phys. Lett.* **80**, 4051 (2002).
- [13] Jana Zaumseil, Takao Someya, Zhenan Bao, Yueh-Lin Loo, Raymond Cirelli, *Appl. Phys. Lett.* **82**, 793 (2003).
- [14] C. D. Dimitrakopoulos, S. Purushothaman, J. Kymissis, A. Callegari, J. M. Shaw, *Science* **283**, 822 (1999).
- [15] T. Masaki, K. Kawata, and T. Masuzawa, *Proc. IEEE Int. Workshop on Micro Electro Mechanical Systems (MEMS'90)*, 21 (1990).
- [16] M. Datta, *IBM J. Res. Develop.* **42**, 655 (1998)
- [17] Ken'ichi Takahata and Yogesh B. Gianchandani, *J. MEMS* **11**, 102 (2002).
- [18] Masuzawa, T., Fujino, M., and Kobayashi, K., *Annals of the CIRP* **34**, 431, (1985).
- [19] Sung Hun Jin, Jin Wook Kim, Chun An Lee, Byung-Gook Park, and Jong Duk Lee, *J. Kor. Phy. Soc.*, **44**, 185, (2004).
- [20] Ioannis Kymissis, Christos D. Dimitrakopoulos, and Sampath Purushothaman, *J. Vac. Sci. Technol.* **B 20(3)**, 956 (2002).